

## New method for measuring 6-DOF micro-displacement based on multi-collimated beams

Liu Lishuang, Lv Yong, Meng Hao, Huang Jiaxing

(School of Instrumentation Science and Optoelectronics Engineering, Beijing Information Science and Technology University, Beijing 100192, China)

**Abstract:** In order to realize in-orbit measurement of the parameters of three-line array satellite-borne CCD camera, a method for measuring 6-DOF (Degree of Freedom) micro-displacement was proposed in this paper. The LED output light with high brightness was collimated and coupled to the input optical fiber. The end of the output fiber was fixed to the movable object to be measured. The fiber outputs were collimated by multiple fiber collimators ( $\geq 4$ ) and captured by multiple area array CCD cameras ( $\geq 4$ ) in the fixed part of the system. The 6-DOF displacement of the measured object was solved according to the position change of the light spot in the CCD image. In order to validate the model of the system and 6-DOF displacement calculation program, the proposed method was theoretically analyzed and simulated. The results show that both the maximum translational error and rotational error of the typical 4-collimation measurement system are under  $10^{-5} \mu\text{m}$  and  $10^{-4}'$  when the translational displacement is less than  $100 \mu\text{m}$  and the rotational displacement is less than  $6'$ . And the limit errors ( $3\sigma$ ) of the translational errors and rotational errors are respectively  $0.9 \mu\text{m}$  and  $0.012'$  when the random quantities of  $-0.5\sim 0.5 \mu\text{m}$  are added to the two coordinate directions of the position of the light spot of the collimators.

**Key words:** 6-DOF; displacement measurement; collimated beam; CCD camera

**CLC number:** TH741 **Document code:** A **DOI:** 10.3788/IRLA201948.0617002

## 采用多准直光束测量六自由度微位移新方法

刘力双, 吕 勇, 孟 浩, 黄佳兴

(北京信息科技大学 仪器科学与光电工程学院, 北京 100192)

**摘 要:** 为实现星载三线阵 CCD 相机的相机参数在轨测量, 提出了一种六自由度微位移测量方法。高亮度 LED 输出光被准直并耦合到输入光纤。输出光纤末端固定在可移动的被测物体上。光纤输出由多个光纤准直器( $\geq 4$ )准直, 并由系统固定部分中的多个区域阵列的 CCD 相机( $\geq 4$ )捕获。根据 CCD 图像中光点的位置变化来求解被测物体的六自由度位移。为了验证系统模型和六自由度位移计算程序, 对该方法进行了理论分析和仿真。结果表明: 当平移位移小于  $100 \mu\text{m}$  且旋转位移小于  $6'$

收稿日期: 2019-01-10; 修订日期: 2019-02-20

基金项目: 北京市自然科学基金(7172035)

作者简介: 刘力双(1981-), 男, 副教授, 博士, 主要从事视觉检测及精密仪器方面的研究。Email: liulishuang@bistu.edu.cn

时,典型的4准直测量系统求解误差小于 $10^{-5}$   $\mu\text{m}$ 和 $10^{-4}'$ 。并且,当准直器的光斑位置的两个坐标方向上添加 $-0.5\sim 0.5$   $\mu\text{m}$ 的随机量时,平移误差和旋转误差的 $3\sigma$ 分别为0.9  $\mu\text{m}$ 和0.012'。

**关键词:** 六自由度; 位移测量; 准直光束; CCD相机

## 0 Introduction

In the field of aerospace, space object acquisition in orbiting spacecraft requires that the relative position and attitude information of the target is accurately acquired in the event that the target's motion and spatial structure are unknown<sup>[1-2]</sup>. In the field of robotics, to measure the end pose of industrial robots is of great significance for robot assembly and robot calibration. For example, in robot assembly, real-time feedback of robot pose is needed to control robot assembly and achieve high-precision positioning<sup>[3]</sup>. In order to check and maintain the accuracy of equipment such as CNC machine tools, it is also necessary to perform accurate measurement in multiple degrees of freedom. At present, scholars at home and abroad have invested in the research of precision measurement technology and devices<sup>[4-5]</sup>. In the field of military, to measure the flight trajectory of missiles is an important means of analyzing the flight status of missiles<sup>[6]</sup>. In addition, the air-floating experimental platform that requires ground experiments on spacecraft and the hull attitude during motion also need to monitor multiple degrees of freedom<sup>[7-8]</sup>.

At present, spatial photogrammetry is mainly based on transmission satellite with a line array CCD camera, in which the latest is satellite-borne three-line array CCD camera, as a payload. In the ground test, the inner orientation parameters of the three-line array CCD mapping camera should be accurately measured to ensure the accuracy of the 3D mapping camera. Nevertheless, the result of the ground test will deviate from the actual value due to weight loss and temperature change when the satellite is in orbit. Consequently the errors are brought to the mapping results. The frequently-used solution for the above-

mentioned problem is to back-calculate the camera parameters through setting some ground control points. Due to the disadvantages of high complexity and time-consuming, this method can merely be used for regular testing rather than real-time monitoring of camera parameters. If the relative 6-DOF displacement between the line array CCD and lens of the mapping camera can be monitored in orbit, the changes of all the parameters of the mapping camera can be solved in real time to improve the mapping accuracy of the mapping satellite<sup>[9-11]</sup>.

The in-orbit monitoring equipment of the satellites should meet the requirements of higher accuracy, fewer parts, simple structure and adjustable installation position, small size, light weight and low power-consumption. However, the existing multi-DOF measurement methods are limited in practical application due to the disadvantages of complex structure and low accuracy. In<sup>[12-13]</sup>, multi-collimated beam is adopted to measure 6-DOF micro-displacement. Unfortunately when the methods are used to measure the relative 6-DOF displacement between the line array CCD and lens of the mapping camera, there is no guarantee of adequate room for installing the parts according to the requirement of the measurement model of the system. In order to solve this problem, a method for measuring 6-DOF micro-displacement based on multi-position unconstrained collimated beam is proposed in this paper.

## 1 Measurement principle

As shown in Fig.1, a 6-DOF displacement measurement system is designed in this paper. The system is composed of a movable part and fixed part. The fixed part is fixed together with a relatively immovable object and the movable part is fixed

together with the object to be measured. The collimated beams from multiple fiber collimators of the movable part are incident on multiple CCD cameras of the fixed part.

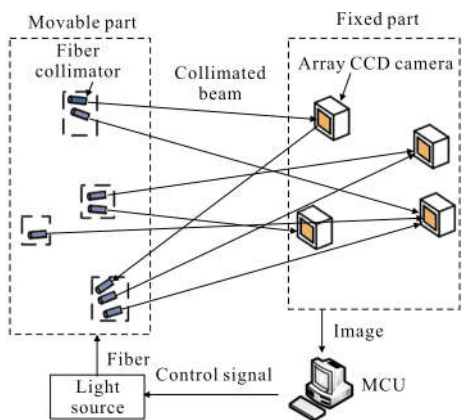


Fig.1 6-DOF displacement measurement system based on unconstrained multi-collimated beam

The implementation of the collimated beam is shown in Fig.2. A high-brightness LED is used as the light source of the system. The beam emitted by the light source is coupled into the input fiber connected to the MEMS optical switch. The optical switch is controlled by the MCU to switch the beam into the output fiber. The collimated beam is emitted by the output fiber through the collimator.

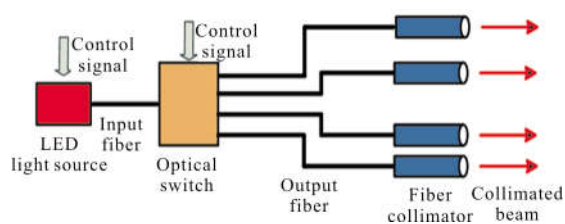


Fig.2 Implementation of the collimated beam

The MCU enables the fiber collimators to shine successively through controlling the switch of the light source and switching of the optical switch, and acquires the light spot image in the corresponding area array CCD. The position of the light spot in the image changes due to the movement of the measured object. The 6-DOF displacement of the measured object is solved according to the position change of the light spot in the image acquired by the area array

CCD.

## 2 Theoretical model of the system

In order to validate the feasibility of the system and solve the 6-DOF displacement, the theoretical model of the system is built in this paper. The process of building model is as follows.

In the spatial model, the collimated beams are regarded as straight lines. And the linear parameters of each collimated beam can be obtained by system calibration. Suppose that there are  $n$  collimated beams. After system calibration, the spatial parameters of the collimated beam  $i$ , as a straight line in the coordinate system of the system, are described by the Eq.(1).

$$\frac{X-X_i}{m_i} = \frac{Y-Y_i}{n_i} = \frac{Z-Z_i}{p_i} \quad (1)$$

Where  $X_i, Y_i, Z_i, m_i, n_i$  and  $p_i$  are known parameters after system calibration.

Suppose the translational displacements in the  $X, Y$  and  $Z$ -directions are respectively  $e, f$  and  $g$ , and the rotational angular displacements around the  $X, Y$  and  $Z$ -axes are respectively  $\alpha, \beta$  and  $\gamma$ .

Through theoretical analysis and software simulation, it can be easily concluded that the final position of the measured object will be different if the order of the displacement of each degree of freedom is different when the measured object moves in multiple degrees of freedom. In the practical 6-DOF measurement system, the order of the displacement must be specified if the displacement of the object is solved on the basis of its final position, otherwise the obtained measurement results are not unique.

Suppose that the order of the displacement is rotation around the  $X$ -axis  $\rightarrow$  rotation around the  $Y$ -axis  $\rightarrow$  rotation around the  $Z$ -axis  $\rightarrow$  translation in the  $X$ -direction  $\rightarrow$  translation in the  $Y$ -direction  $\rightarrow$  translation in the  $Z$ -direction. The straight line equation after movement can be obtained by the Eq.(2).

$$\frac{X-X'_i}{m_i} = \frac{Y-Y'_i}{n_i} = \frac{Z-Z'_i}{p_i} \quad (2)$$

The relationship between the line parameters  $(X'_i, Y'_i, Z'_i)$  and  $(X_i, Y_i, Z_i)$  can be described by the Eq.(3).

$$\begin{bmatrix} X'_i \\ Y'_i \\ Z'_i \\ 1 \end{bmatrix}^T = \begin{bmatrix} X_i \\ Y_i \\ Z_i \\ 1 \end{bmatrix}^T \begin{bmatrix} 1 & 0 & 0 & 0 \\ 0 & \cos\alpha & \sin\alpha & 0 \\ 0 & -\sin\alpha & \cos\alpha & 0 \\ 0 & 0 & 0 & 1 \end{bmatrix} \quad (3)$$

$$\begin{bmatrix} \cos\beta & 0 & -\sin\beta & 0 \\ 0 & 1 & 0 & 0 \\ \sin\beta & 0 & \cos\beta & 0 \\ 0 & 0 & 0 & 1 \end{bmatrix} \begin{bmatrix} \cos\chi & \sin\chi & 0 & 0 \\ -\sin\chi & \cos\chi & 0 & 0 \\ 0 & 0 & 1 & 0 \\ 0 & 0 & 0 & 1 \end{bmatrix} \begin{bmatrix} 1 & 0 & 0 & 0 \\ 0 & 1 & 0 & 0 \\ 0 & 0 & 1 & 0 \\ e & f & g & 1 \end{bmatrix}$$

It can be concluded that

$$X'_i = [X_i \cos\beta + (Y_i \sin\alpha + Z_i \cos\alpha) \sin\beta] \cdot \cos\chi - (Y_i \cos\alpha - Z_i \sin\alpha) \sin\chi + e \quad (4)$$

$$Y'_i = [X_i \cos\beta + (Y_i \sin\alpha + Z_i \cos\alpha) \sin\beta] \cdot \sin\chi + (Y_i \cos\alpha - Z_i \sin\alpha) \cos\chi + f \quad (5)$$

$$Z'_i = (Y_i \sin\alpha + Z_i \cos\alpha) \cos\beta - X_i \sin\beta + g \quad (6)$$

Substituting the linear vector end point coordinate  $((m_i + X_i), (n_i + Y_i), (p_i + Z_i))$  into the Eq.(3), the end point of the vector end point coordinate after the 6-DOF micro-displacement  $((m_i + X_i)', (n_i + Y_i)', (p_i + Z_i)')$  can be obtained. The relationship between the vector parameters of the straight line  $(m'_i, n'_i, p'_i)$  and  $(m_i, n_i, p_i)$  can be described by the Eq.(7).

$$\begin{bmatrix} m'_i \\ n'_i \\ p'_i \end{bmatrix}^T = \begin{bmatrix} (m_i + X_i)' - X'_i \\ (n_i + Y_i)' - Y'_i \\ (p_i + Z_i)' - Z'_i \end{bmatrix} \quad (7)$$

Then  $m'_i, n'_i$  and  $p'_i$  can be respectively obtained by the Eqs.(8), (9) and (10).

$$m'_i = \cos(\chi) \times (\sin(\beta) \times (\cos(\alpha) \times (Z_i + p_i) + \sin(\alpha) \times (Y_i + n_i)) + \cos(\beta) \times (X_i + m_i)) - \sin(\chi) \times (\cos(\alpha) \times (Y_i + n_i) - \sin(\alpha) \times (Z_i + p_i)) + \sin(\chi) \times (Y_i \times \cos(\alpha) - Z_i \times \sin(\alpha)) -$$

$$\cos(\chi) \times (X_i \times \cos(\beta) + \sin\beta \times (Z_i \times \cos(\alpha) + Y_i \times \sin(\alpha))) \quad (8)$$

$$n'_i = \sin(\chi) \times (\sin(\beta) \times (\cos(\alpha) \times (Z_i + p_i) + \sin(\alpha) \times (Y_i + n_i)) + \cos(\beta) \times (X_i + m_i)) + \cos(\chi) \times (\cos(\alpha) \times (Y_i + n_i) - \sin(\alpha) \times (Z_i + p_i)) + \cos(\chi) \times (Y_i \times \cos(\alpha) - Z_i \times \sin(\alpha)) - \sin(\chi) \times (X_i \times \cos(\beta) + \sin\beta \times (Z_i \times \cos(\alpha) + Y_i \times \sin(\alpha))) \quad (9)$$

$$p'_i = \cos(\beta) \times (\cos(\alpha) \times (Z_i + p_i) + \sin(\alpha) \times (Y_i + n_i)) - \sin(\beta) \times (X_i + m_i) + X_i \times \sin(\beta) - \cos(\beta) \times (Z_i \times \cos(\alpha) + Y_i \times \sin(\alpha)) \quad (10)$$

The light spot image of the collimated beam in the area array CCD is acquired and processed by the MCU after the measured object moves. Thereby the image coordinate of the light spot in the CCD is solved. In the coordinate system of the measurement system, according to the calibrated transformation relationship between the image coordinate and the system coordinate, the 3D coordinate of the light spot of the collimated beam  $i$  can be obtained.

Change the Eq.(2) into the Eq.(11), namely,

$$\begin{cases} (X - X'_i)n'_i - (Y - Y'_i)m'_i = 0 \\ (X - X'_i)p'_i - (Z - Z'_i)m'_i = 0 \end{cases} \quad (11)$$

By introducing the coordinate  $(X''_i, Y''_i, Z''_i)$  into the parameter equation of the collimated beam, two equations with six unknown variables including  $e, f, g, \alpha, \beta$  and  $\gamma$  can be obtained. With  $n$  collimated beams,  $2n$  equations can be obtained to be an equation set. When  $n \geq 4$ , the equation set is an overdetermined nonlinear equation set. Through solving the equation set by fsolve function of MATLAB, the 6-DOF displacement, namely  $e, f, g, \alpha, \beta$  and  $\gamma$ , can be obtained.

The spatial linear parameters of the collimated beam and the transformation relationship between the image coordinate system of the CCD and the coordinate system of the measurement system should be calibrated by the system calibration.

### 3 Hardware configuration

The LED light source and optical switch (SW1×

4-62N-07-17, SERCALO) of the system are shown in Fig.3, and the fiber collimator of the system is shown in Fig.4 (customized). Stability testing of the system based the collimated beam is shown in Fig.5, and the light spot image collected by the CCD camera (Guppy F-146B, AVT) is shown in Fig.6. The stability experiment of the system based on the collimated beam was carried out and the single-DOF displacement was measured by the system in Ref.[16]. The experimental results show that the standard deviation of single-direction measurement stability of the system is about 0.031 pixels (0.15 μm). The limit error of single-DOF displacement is less than 0.5 μm.

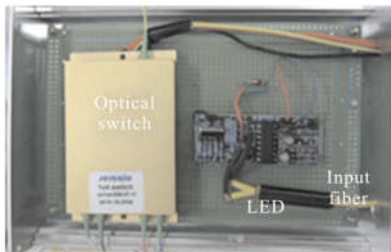


Fig.3 LED light source and optical switch

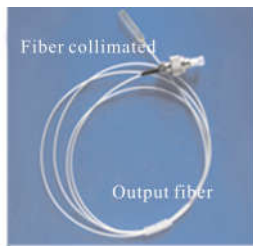


Fig.4 Fiber collimator



Fig.5 Stability testing of the system based on the collimated beam



Fig.6 Light spot image collected by the CCD

## 4 Software simulation

### 4.1 Software simulation method

Some straight lines are used to simulate the collimated beams in the simulation software. The position change of the light spot of the incident collimated beam in the area array CCD resulting from the multi-DOF displacement of the measured object is simulated by using AutoCAD. Introducing the position of the light spot after movement into the program for calculating the 6-DOF displacement, the displacement in each degree of freedom is solved. The measurement accuracy of the system can be analyzed by comparing the solved displacement with the one obtained by simulation software.

In the process of implementing software simulation, random errors in a certain range are added to the center of the light spot image in the CCD after movement in order to analyze the influence of the random errors of the optical collimation system on the measurement accuracy of the system. In order to simplify the calculation and make the calculation results more intuitive, the models of four spatial lines shown in Fig.7 are built in the simulation software. As shown in Fig.7, all the four lines intersect at the coordinate origin (0, 0, 0) and the CCD cameras are located at C1, C2, C3 and C4. In AutoCAD, the 3-DOF translational displacement and rotational displacement around the coordinate origin of the four

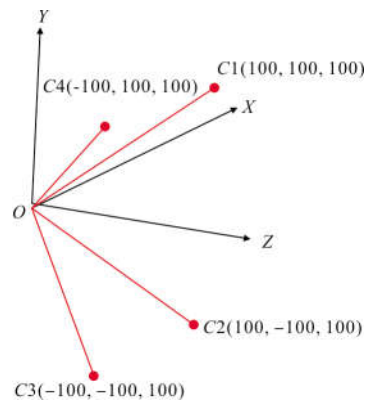


Fig.7 Model of the system based on 4-collimated beam

spatial lines are carried out. The linear parameters after movement are introduced into the displacement calculation program of the model of the system to solve the 6-DOF displacement. The maximum translational displacement and rotational displacement are respectively set to 100 μm and 6' when this system is applied to measure spatial loads in orbit.

**4.2 Simulation experiment of single-DOF displacement**

In order to validate the model of the system, a simulation experiment is carried out to make the measured object move at a certain degree of freedom in simulation software. The simulation results are shown in Tab.1. It can be seen from Tab.1 that a single-DOF displacement can be accurately measured by the model of the system.

**Tab.1 Simulation results of single-DOF displacement**

No.	X/μm	Y/μm	Z/μm	α/(')	β/(')	γ/(')
Displacement	100	0	0	0	0	0
1 Calculation	100	0	0	0	0	0
Error	0	0	0	0	0	0
Displacement	0	100	0	0	0	0
2 Calculation	0	100	0	0	0	0
Error	0	0	0	0	0	0
Displacement	0	0	100	0	0	0
3 Calculation	0	0	100	0	0	0
Error	0	0	0	0	0	0
Displacement	0	0	0	6	0	0
4 Calculation	0	0	0	6	0	0
Error	0	0	0	0	0	0
Displacement	0	0	0	0	6	0
5 Calculation	0	0	0	0	6	0
Error	0	0	0	0	0	0
Displacement	0	0	0	0	0	6
6 Calculation	0	0	0	0	0	6
Error	0	0	0	0	0	0

**4.3 Simulation experiment of multi-DOF displacement**

In the simulation software, a simulation experiment is carried out to make the measured object move at multiple degrees of freedom. The influence of the displacement order on the results is not temporarily taken into consideration. Suppose the order of the displacement is translation in the X-direction -> translation in the Y-direction -> translation in the Z-direction -> rotation around the X-axis -> rotation around the Y-axis -> rotation around the Z-axis. The simulation results are shown in Tab.2. It can be seen

**Tab.2 Simulation results of multi-DOF displacement**

No.	X/μm	Y/μm	Z/μm	α/(')	β/(')	γ/(')
Displacement	100	100	100	0	0	0
1 Calculation	100	100	100	0	0	0
Error	0	0	0	0	0	0
Displacement	0	0	0	6	6	6
2 Calculation	0	0	0	6	6	6
Error	0	0	0	0	0	0
Displacement	100	0	0	6	0	0
3 Calculation	100	0	0	6	0	0
Error	0	0	0	0	0	0
Displacement	0	100	0	0	6	0
4 Calculation	0	100	0	0	6	0
Error	0	0	0	0	0	0
Displacement	0	0	100	0	0	6
5 Calculation	0	0	100	0	0	6
Error	0	0	0	0	0	0
Displacement	100	100	0	6	6	0
6 Calculation	100	100	0	6	6	0
Error	0	0	0	0	0	0
Displacement	100	0	100	6	0	6
7 Calculation	100	0	100	6	0	6
Error	0	0	0	0	0	0
Displacement	100	100	100	6	6	6
8 Calculation	100	100	100	6	6	6
Error	0	0	0	0	0	0

from Tab.2 that multi-DOF displacement can be measured by the model of the system. Combined with Tab.1 and Tab.2 and a large number of simulation experiments, the error of solving the equation are under  $10^{-5} \mu\text{m}$  and  $10^{-4}'$  when the translational displacement and the rotational displacement are respectively less than  $100 \mu\text{m}$  and  $6'$ . Consequently, the simulation experiment shows that multi-DOF displacement can be accurately measured by the model of the system.

### 5 Simulation experiment of the influence of random errors of optical collimation system

In the practical optical collimation system, there exist random errors in the light spot center coordinate of the image in the CCD due to the instability of the light source, beam drift, the noise of the CCD camera and other factors. Hence the influence of the random errors on the 6-DOF displacement must be considered in the measurement system. In order to learn the influence of the random errors of the optical collimation system on the measurement accuracy of the 6-DOF measurement system, a random quantity of  $-0.5 \mu\text{m}$  to  $0.5 \mu\text{m}$  is added to the  $X$  and  $Y$ -coordinate of the light spot center of the image in the CCD to simulate and analyze the errors in the measurement results resulting from the errors of the optical collimation system. The results of the simulation experiment are shown in Tab.3. It can be seen from Tab.3 that the limit errors ( $3\sigma$ ) of the three translational errors and three rotational errors are not more than  $0.9 \mu\text{m}$  and  $0.012'$  respectively. The experimental results show that the measurement errors of the system are smaller when the random errors of the optical collimation system are taken into consideration.

**Tab.3 4-collimated model errors ( $0.5 \mu\text{m}$  measurement errors)**

No.	$X/\mu\text{m}$	$Y/\mu\text{m}$	$Z/\mu\text{m}$	$\alpha/(')$	$\beta/(')$	$\gamma/(')$
1	100.0	100.2	99.9	6.000	6.000	5.989
2	99.9	100.1	99.9	6.003	6.001	6.000
3	100.2	99.8	100.1	5.997	5.996	5.994
4	99.9	100.0	99.8	5.998	6.002	6.002
5	100.0	100.2	99.8	6.002	6.001	5.999
6	100.1	99.5	100.1	5.994	6.001	5.997
7	99.7	99.5	99.8	5.993	6.007	6.002
8	99.9	99.6	100.0	5.996	6.000	6.000
9	100.1	99.2	100.1	5.988	5.998	6.001
10	99.9	100.1	100.0	6.000	6.002	6.010
...	...	...	...	...	...	...
100	100.1	99.7	100.0	5.993	5.997	6.000
$\sigma$	0.3	0.3	0.1	0.004	0.004	0.004
$3\sigma$	0.9	0.9	0.3	0.012	0.012	0.012

### 6 Factors that influence the measurement accuracy

In Ref.[17], the influence of the CCD parameters on the measurement accuracy of the system was studied. The results show that the displacement cannot be accurately measured by the model of the system when the quantity of the CCD camera is one, two or three. Similarly when there are four CCD cameras arranged collinearly in the system, the displacement cannot be accurately measured by the model of the system. By comparison, the displacement can be accurately solved by the model of the system when the four cameras are arranged in square. Hence in order to ensure the accuracy of the system, at least four cameras are required in the system and they cannot be arranged collinearly or approximately collinearly.

### 7 Conclusions

A novel method for measuring 6-DOF micro-displacement on the basis of multi-collimated beam is

proposed in this paper. The proposed method has the advantages of fewer parts, simple structure, small size, light weight and low power-consumption. And the positions of the fiber collimators and area array CCD cameras are unconstrained in the model of the system, so it is easy to install and adjust the system. The proposed method can be used to measure 6-DOF micro-displacement based on three-line array satellite-borne CCD camera, and can also be used to measure multi-DOF displacement in other applications.

### References:

- [1] Yang Ning, Shen Jingshi, Zhang Jiande, et al. Autonomous measurement of relative attitude and position for spatial non-cooperative spacecraft based on stereo vision [J]. *Optics and Precision Engineering*, 2017, 25(5): 1331-1339. (in Chinese)
- [2] Zhang Tieyi, Xue Jianping, Sun Chaojiao, et al. A vision-based location method for spacecraft docking [J]. *Flight Dynamics*, 2016, 34(1): 68-71.
- [3] Zhang Xu, Wei Peng. Monocular vision calibration method of the stereo target for robot pose measurement [J]. *Infrared and Laser Engineering*, 2017, 46(11): 1117005. (in Chinese)
- [4] Du Zhengchun, Yangjianguo, Feng Qibo. Research status and trend of geometrical error measurement of CNC machine tools [J]. *Aeronautical Manufacturing Technology*, 2017(6): 34-44. (in Chinese)
- [5] Li Xinghua, Xing Yanlei, Fang Fengzhou, et al. Multi-parameter measurement method based on combined surface reference [J]. *Infrared and Laser Engineering*, 2018, 47(7): 0717001. (in Chinese)
- [6] Zhang Yuan, Wang Zhiqian, Qiao Yanfeng, et al. Attitude measurement method research for missile launch [J]. *Chinese Optics*, 2015, 8(6): 997-1003. (in Chinese)
- [7] Liu Yuhang, Gu Yingying, Li Ang, et al. Pose visual measurement of the flotation experiment platform [J]. *Infrared and Laser Engineering*, 2017, 46 (10): 1017005. (in Chinese)
- [8] Ma Qingkun, Qiao Yanfeng, Wang Xiaofeng, et al. Real-time measurement of dynamic horizontal attitudes of ships based on optical method [J]. *Chinese Optics*, 2012, 5(2): 189-193. (in Chinese)
- [9] Lv Yong, Feng Qibo, Sun Shijun, et al. Feasibility analysis of on-orbit intersection angle monitoring for three-line-array mapping camera [J]. *Infrared and Laser Engineering*, 2012, 41(12): 3390-3396. (in Chinese)
- [10] Wang Renxiang, Wang Jianrong, Zhao Fei, et al. Dynamic calibrating of three-line-array CCD camera in satellite photogrammetry using ground control point [J]. *Journal of Earth Sciences & Environment*, 2006, 28(2): 1-5. (in Chinese)
- [11] Hu Xin, Cao Xibin. Analysis on precision of stereo mapping microsatellite using three-line array CCD images [J]. *Journal of Harbin Institute of Technology*, 2008, 40 (5): 695-699. (in Chinese)
- [12] Lv Yong, Feng Qibo, Liu Lishuang, et al. Six-degree-of-freedom measurement method based on multiple collimated beams [J]. *Infrared and Laser Engineering*, 2014, 43(11): 3597-3603. (in Chinese)
- [13] Lv Yong, Sun Peng, Liu Lishuang, et al. A roll angle measurement method based on dual CCDs [J]. *Optical Technique*, 2013, 39(5): 477-480. (in Chinese)
- [14] Lv Yong. Study on position-pose measurement method and application using multiple collimated beams [D]. Beijing: Beijing Jiaotong University, 2015. (in Chinese)
- [15] Lv Yong, Feng Qibo, Liu Lishuang, et al. Application of optical switch in precision measurement system based on multi-collimated beams [J]. *Measurement*, 2015, 61 (61): 216-220. (in Chinese)
- [16] Liu Lishuang, Lv Yong, Lang Xiaoping, et al. Research on space-borne optical collimation system [C]//Proceedings of SPIE -The International Society for Optical Engineering, 2011, 8321: 153.
- [17] Liu Lishuang, Lv Yong, Meng Hao, et al. Influence of CCD parameters on measurement accuracy in 6-DOF measurement method [J]. *Laser Journal*, 2018, 39(1): 89-92. (in Chinese)